Probing diameter-selective solubilisation of carbon nanotubes by reversible cyclic peptides using molecular dynamics simulations†

S. R. Friling, R. Notman and T. R. Walsh*

Received 19th August 2009, Accepted 15th October 2009
First published as an Advance Article on the web 6th November 2009
DOI: 10.1039/b9nr00226j

Molecular dynamics simulations are used to explore the encapsulation behaviour of reversible cyclic peptides when adsorbed onto single-walled carbon nanotubes (CNTs) in aqueous solution. Our findings suggest that CNT encapsulation *via* cyclisation of a single peptide chain is relatively less likely, compared with encapsulation *via* two-chain complexes. These two-chain complexes comprise pairings of the motifs identified for single-chain adsorption. Our simulation data are compared with existing experimental findings [A. Ortiz-Acevedo *et al*., *J. Am. Chem. Soc.*, 2005, 127, 9512], for relevant CNT diameters, and are found to be consistent with the experimental results. Our data help to explain the limited diameter selectivity reported by Ortiz-Acevedo *et al*. These findings should help in the optimisation and future design of peptides capable of enhanced selectivity for specific CNT diameters.

Introduction

There are myriad of potential applications of single-walled carbon nanotubes (CNTs) ranging from biological applications such as ion channel blockers[1] and artificial muscle[2] to novel medicinal applications such as new drug screening tools,[3] sensors[4–6] and drug-delivery vehicles.[7] However, when added to water CNTs readily aggregate into bundles due to being highly hydrophobic; problematic where biological systems are concerned, as single, dispersed nanotubes (rather than bundles) are typically required for such biological and medical applications.[2–4] The search for strategies for CNT separation, selective for tube size and/or chirality, is ongoing; in particular for those strategies that do not require the use of surfactants[8] or other additives that may present a hazard to living systems.

Many strategies for size-selective solubilisation of CNTs have focussed on utilisation of non-covalent interactions, making use of peptides,[9–15] polymers,[16,17] surfactants,[18,19] DNA,[20] or small molecules[21] to selectively disperse CNTs. One such strategy was recently reported by Ortiz-Acevedo *et al*.,[12] where reversible cyclic peptides were shown to confer limited selectivity in CNT diameter when solubilised. In the reduced form, these peptides have a linear architecture, containing alternating arrangements of L- and D-amino acids (in this case Ala and Lys), with the N- and C-termini derivatised with thiol groups. Upon oxidation it is supposed that these terminating groups support the reversible formation of a disulfide bond between the chain ends, yielding a cyclic architecture. These authors demonstrated that cyclisation of these peptides, *in the presence of the CNTs* in water, led to diameter-selective CNT solubilisation. This study also showed that treatment with uncyclised (linear) peptides did not lead to effective CNT dispersion, nor did addition of pre-cyclised peptide to the CNTs in water. However, the limited diameter selectivity behaviour reported in this work cannot be explained *via* a simple structural model alone, where the peptide forms a circularly-wrapped conformation when adsorbed on the CNT surface. Nor can this model explain how such a peptide can solubilise CNTs where the circular cross-section arc-length of the tube is greater than the contour length of the peptide. The authors hypothesised on the formation of polymerised (helical) arrangements of these peptides (at sufficiently high local concentrations) as a possible cause.

In contrast, a different encapsulation mode is presented by Nish *et al*.[22] As part of a comprehensive experimental/theoretical study of the effect of polymer-wrapping of nanotubes, these authors reported dispersion of CNTs in organic solvents *via* adsorption of poly(9,9-dioctylfluorenyl-2,7-diyl) (referred to as PFO). Interestingly, these authors also reported molecular dynamics (MD) simulation data of oligomeric chains of PFO interacting with the CNT surface, suggesting that tube encapsulation could be attributed not to one oligomer alone, but to several oligomers that aggregated around the CNT. Their findings suggested that an integer number of PFO oligomers was associated with CNT encapsulation for a small range of CNT diameters, with this number incrementing sharply at critical tube diameters.

Despite the considerable growth in the experimental study of the peptide–CNT interface, simulation studies remain few in number.[23–29] In our previous studies,[23] we reported results of MD simulations of single-walled CNTs interacting with 'binder' and 'non-binder' aptamers, as identified by Wang *et al*.[9] Our results confirmed experimental observations[9] of relative binding affinity for the systems studied. We also reported MD simulations probing the effects of residue mutation on binding affinity (and therefore solubilisation activity) for a CNT-binding peptide,[29] where tryptophan was mutated for either phenylalanine or tyrosine; these results broadly agreed with the experimental findings of Xie *et al*.[30] and Salzmann *et al*.[31]

No simulation studies of the adsorption of reversible cyclic peptides onto CNT surfaces have yet been reported. In this work,

Dept. of Chemistry and Centre for Scientific Computing, University of Warwick, Coventry, CV4 7AL, U.K. E-mail: t.walsh@warwick.ac.uk
† Electronic supplementary information (ESI) available: Table S1 and Figs. S2–S7. See DOI: 10.1039/b9nr00226j

in order to further our understanding of the interactions at the peptide–CNT interface in general, and to explore the diameter selectivity of the solubilisation of CNTs by reversible cyclic peptides in particular, we present results of MD simulations of the aqueous peptide–CNT interface. Specifically, we investigated the selectivity of the same cyclic peptides used by Ortiz-Acevedo *et al.*[12] for solubilisation of CNTs of different diameter (ranging from 0.75 nm to 1.45 nm, inclusive of van der Waals radius). It is clear from the experiments of Ortiz-Acevedo *et al.*[12] that the formation of disulfide bonds in the peptide–CNT solution is crucial for CNT dispersal. However, there is no direct indication that these disulfide bonds must be intra-molecular in origin. To this end, and in light of the simulations reported by Nish *et al.*,[22] we have considered several different scenarios; encapsulation of the CNT *via* a single peptide that can support an intra-molecular disulfide bond, CNT encapsulation *via* two peptides that can make an effective pseudo-cyclised chain by formation of inter-molecular disulfide bonds, and finally, CNT encapsulation *via* two chains that can helically-wrap the CNT again by formation of an inter-molecular disulfide bond.

Since the experiments of Ortiz-Acevedo *et al.*[12] showed that for best performance the peptides had to be cyclised in the presence of the CNTs (*e.g.* addition of pre-cyclised peptide to the CNTs in solution did not yield good dispersion), in our work the peptides are treated in their un-cyclised (linear) form, without the presence of any disulfide bonds. Our prediction of the likelihood of disulfide bond formation is based on the stability of peptide conformations that maintain close sulfur–sulfur non-bonded separations. We propose that un-cyclised peptide conformations that cannot sustain close sulfur–sulfur non-bonded separations are not likely to form disulfide bonds. In each of the three cases outlined above, we have sought to identify peptide conformations that could conceivably *support* formation of disulfide bonds, for the range of CNT diameters explored in the experimental study.

Methods

Following Ortiz-Acevedo *et al.*,[12] two reversible cyclic peptides are considered in this work; R_1-Y(^{D}AK)$_4{}^D$AQ-NH-R_2 (denoted RC5) and R_1-Y(^{D}AK)$_6{}^D$AQ-NH-R_2 (denoted RC7). The terminating groups R_1 and R_2 are defined as the fragments $HSCH_2CO$– and –$NHCH_2CH_2SH$ respectively. RC5 and RC7 differ only in the length of the central segment of the chain. These peptides were generated using the protein builder in the TINKER package.[32] The builder in this package was modified to permit construction of the customised terminating groups R_1 and R_2. A modified version of the ffG43a1 forcefield,[33] implemented in the GROMACS[34–36] package, was edited to include all bonds, angles, dihedrals and improper angles present in these customised terminating groups. Hydrogens attached to the sulfur atoms in R_1 and R_2 were defined atomistically in the force field.

Several different classes of systems were modelled, the first being the peptide in water, without the presence of a nanotube. In this case, a single peptide (one of either RC5 or RC7) was placed in a periodic cubic box (with side length of around 6.1 nm for RC5, and 7.5 nm for RC7). The system was then solvated using the SPC water model[37] and chlorine ions were added to ensure overall charge neutrality of the cell. Molecular dynamics in the canonical (NVT) ensemble was used to explore peptide conformation in solution, employing the leap-frog algorithm to integrate Newton's equations of motion with a time-step of 1 fs. The temperature was held fixed at 300 K using the Nosé–Hoover thermostat.[38–40] Long-range electrostatics were handled using the particle-mesh Ewald[41] approach with a cut-off of 1.2 nm. The system was equilibrated for 2 ns, followed by a 10 ns production run, with frames saved every ps.

The second system we constructed comprised a single CNT placed in a periodic rectangular simulation cell, along with one peptide (either RC5 or RC7), and solvated using SPC water. Again, the *NVT* ensemble was used, with simulation conditions as specified above. Box dimensions perpendicular to the long axis of the CNT were adjusted to yield the correct SPC water density at a temperature of 300 K in the bulk water region, but were roughly 8 nm × 8 nm. Molecular structures of non-metallic CNTs of length between roughly 7.5 and 8.0 nm were generated using the tubeBASH[42,43] script, with atom-to-atom diameters, D_a, ranging from approximately 0.45 nm to 1.25 nm in intervals of 0.1 nm. The (n, m) indices are given in Table S1 of the ESI.† We point out here that the tube diameters reported by Ortiz-Acevedo *et al.*[12] *are inclusive of* van der Waals radii (denoted herein as D_v); we converted between the two using a van der Waals diameter of 3.5 Å for carbon (*e.g.* D_a of 0.45 nm yields $D_v = 0.8$ nm). Periodic boundary conditions ensured that the CNTs modelled here were of infinite length. Different general types of starting configuration were used for each tube and peptide combination; a 'cross-bar' geometry (where the extended peptide was placed close to the CNT such that the long axis of the peptide was rotated 90° to the CNT long axis), a 'co-linear' geometry (where the long-axis of the extended peptide roughly coincided with the CNT long axis) and, for selected CNTs, a 'cyclised-wrap' geometry. In this last case, the peptide backbone was constructed in a circular arrangement, and placed on the CNT such that the chain wrapped completely around the CNT and the sulfur atoms at either end of the chain were spaced roughly 4–4.5 Å apart. For this cyclised-wrap geometry the diameters explored for RC5 were D_a = 0.45–0.85 nm (the upper value represents the limiting tube diameter that can be wrapped by RC5); and similarly for RC7, the range of D_a from 0.75 nm to 1.25 nm was considered. Two production runs were obtained for each peptide/tube combination for each of these three initial configurations. For the cross-bar and co-linear geometries, production runs lasted between 7 and 11 ns. For the cyclised-wrap geometry, production runs were shorter, and depended on the time taken for the non-bonded sulfur–sulfur contact to retract (*vide infra*); generally these production runs were continued for at least 1 ns beyond the point of sulfur–sulfur retraction. Examples of each type of starting configuration are shown in Fig. 1.

In addition, to explore the cyclised-wrap geometry further, a 'bonded-wrapped' geometry was also created in the case of the RC5 peptide on the D_a = 0.75 nm tube. In this case, the peptide was placed in a cyclised-wrap geometry with the sulfur atoms at either end of the chain permanently bonded (*i.e.* configured in a disulfide bond), such that the peptide could not unwrap from the tube. After 2 ns run time, the topology files were amended to cut this disulfide bond; hydrogens were added manually to each sulfur atom, and the simulations re-started. Again, the same simulation conditions were used as stated above. As in the cyclised-wrap cases, length of production run depended on the time taken for the sulfur–sulfur non-bonded contact to retract.

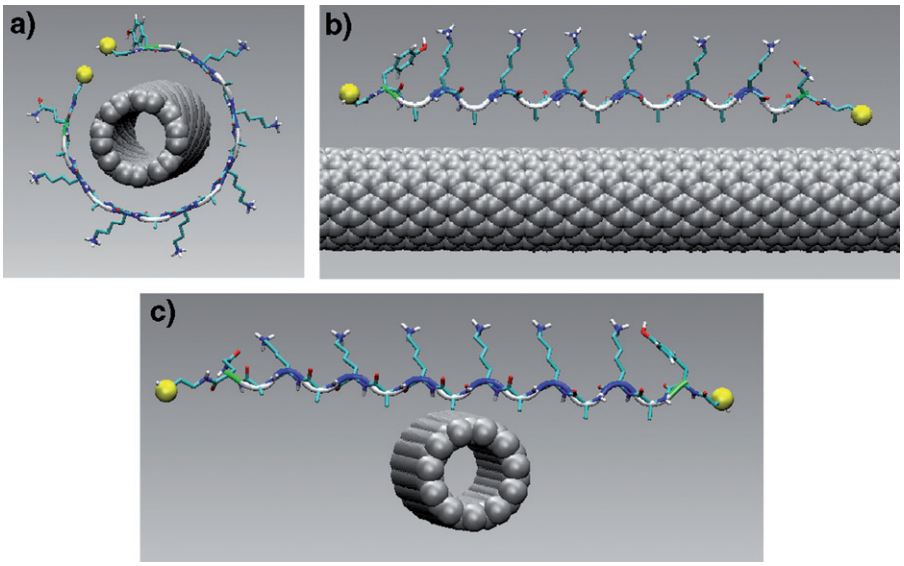

Fig. 1 Example snapshots of the three types of starting configuration used in the simulations of a single peptide adsorbed onto the CNT. (a) cyclised-wrap, (b) co-linear, (c) cross-bar. The relative size of the sulfur atoms (yellow) is increased for clarity.

In the third type of system constructed, two peptide chains (two of either RC5 or RC7) were placed on a single CNT under aqueous conditions. Details of the periodic cell dimensions were similar to those given for the single peptide–CNT simulations. These two-chain systems were started in three different types of initial configuration. The first was a 'dimer' structure, where the two chains were each constructed in a roughly semi-circular (half-wrap) arrangement, and the thiol chain ends—either the 'head' (Tyr end) or 'tail' (Gln end)—of each peptide semi-circle were positioned closely such that the two chains encircled the nanotube. The second was a 'helix', where each peptide chain was formed into a helix (or a fragment of a helix, depending on the CNT radius), such that each chain alone could partially wrap the nanotube; these two partial helices were then placed in an end-to-end fashion on the CNTs. The last initial configuration was the 'double-wrapped' geometry, with two single cyclised-wrap peptides arranged side-by-side on the CNT. This final initial geometry was studied to explore if any additional stabilisation effects arose due to having two chains on the peptide surface in general, (since they are started in neither a dimer or helix arrangement). For the dimer and helix configurations, runs were done for each peptide and the 0.45, 0.75 and 1.15 nm CNT diameters (D_a), and two production runs were generated in each case. For the 'double-wrapped' configuration, we only explored the case of RC7 chains adsorbed on a $D_a = 0.75$ nm CNT; three production runs were generated in this case. Examples of each type of two-chain starting configuration are shown in Fig. 2.

A combination of structural metrics was used to characterise the peptide–nanotube interface, principally: the non-bonded distance between sulfur atoms, the distance between the peptide backbone atoms and the CNT surface, and the percentage of radial coverage of the peptide around the CNT *i.e.* the extent of wrapping. In the latter analysis, we calculated a set of vectors in the xy plane (with the z-axis pointing along the long axis of the CNT) from the CNT centre to each peptide backbone atom, including the sulfur atoms at the chain ends, such that each vector was normal to the tube surface. The vector passing through the sulfur atom in the R1 terminus group was always aligned with the y-axis, and formed our reference vector. For all other backbone atoms, the angle between this reference vector and each atom vector was calculated. A histogram was then constructed of these angles, for each frame over the entire production trajectory, with a bin width of 10°. The percentage of radial coverage was calculated for each frame, as the number of bins in the histogram that contained at least one backbone atom, divided by the number of bins in total (36 bins in total). A coverage of 100% signified perfect, idealised encapsulation of the CNT.

Based on our simulations, we considered that a peptide–CNT complex was no longer capable of supporting encapsulation when the relevant sulfur–sulfur non-bonded distance had retracted to over 15 Å, and/or the percentage of radial coverage had dropped to 65%. These thresholds were chosen because we

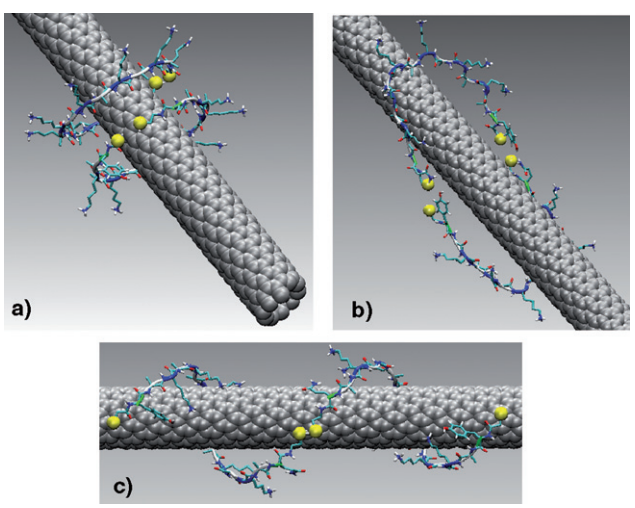

Fig. 2 Example snapshots of the three types of starting configuration used in the simulations of two peptides adsorbed onto the CNT. (a) Two cyclised-wrap peptides, (b) dimer configuration, (c) helix configuration. The relative size of the sulfur atoms (yellow) is increased for clarity.

generally did not note a good deal of evidence showing that encapsulation could be sustained once beyond these points. In our analysis of the relative stability of the configurations described above, we measured how long a given system could sustain *both* the relevant sulfur–sulfur non-bonded close contact (< 15 Å) *and* a radial coverage of 65% or greater. Simultaneous satisfaction of both these criteria ensured a thorough characterisation of tube encapsulation as described in the experiments of Ortiz-Acevedo *et al.*,[12] since a high coverage could be maintained in the absence of the necessary sulfur–sulfur contacts, and conversely, the sulfur–sulfur contacts could be maintained in the absence of the necessary radial coverage. All images of molecular snapshots were generated using VMD;[44] in all cases water molecules were omitted for the purpose of clarity.

Results

Peptide-water simulations

A range of initial configurations for the simulations of the peptide in water were investigated including a fully-extended geometry and a circular configuration (where the sulfur atoms of the chain ends were within 4–4.5 Å of each other). Regardless of starting configuration, almost all cases formed a β-hairpin turn part way along the chain, such as shown in Fig. 3(a). The definition of a β-turn used here is based on the close (< 7 Å) non-bonded separation of C^{α} carbons separated by three peptide bonds, since hydrogen bonding did not always appear to be present in these β-turns. For example, in the RC7 structure shown in Fig. 3(a), over the last 1 ns of production run the 10th and 13th α-carbons maintained an average separation of 5.2 Å, and spent the entire time separated by less than 7 Å. Overall, these peptide–water simulations suggested that there may be some energetic penalty to adopting a circular conformation around a CNT, since for a single RC5 or RC7 peptide to completely wrap around a CNT, β-turns could not be adopted along the backbone, except for wrapping of CNTs of very narrow diameter.

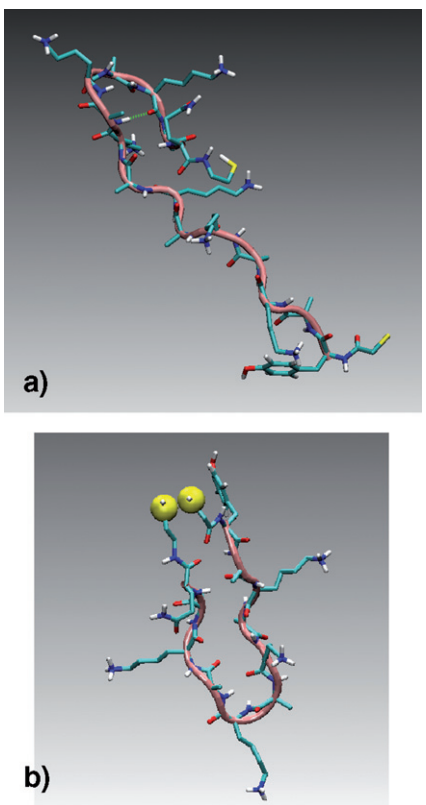

Fig. 3 (a) Snapshot of a typical conformation of the RC7 peptide in aqueous solution (without the presence of a CNT), showing a β-turn. In this case, a hydrogen bond is present and is indicated by the dashed green line. (b) Snapshot of the conformation of the RC5 chain resulting from a simulation where the intra-chain sulfur–sulfur distance was constrained.

In particular, for the circular initial configurations, out of three simulations run, two of these rapidly formed β-hairpin structures, while the other resulted in an extended configuration. To explore this further, simulations were run of the circular configuration, where the sulfur atoms at either end of the chain were defined as permanently-bonded for the first nanosecond of production simulation, with this bond released thereafter. After breaking the disulfide bond, a β-hairpin structure formed and remained intact. As an alternative, we also performed simulations starting in the circular configuration, but with the sulfur atoms frozen in space for the first nanosecond and released thereafter. In Fig. 3(b) the resulting conformation of the RC5 chain after 1 ns is shown, clearly indicating the narrow gap between the chain strands. After release of the sulfur atoms, again, β-turn formation resulted. These data may explain why Ortiz-Acevedo *et al.*[12] failed to observe solubilisation of CNTs by addition of pre-cyclised peptide, since our simulation results suggest that the gap between the peptide chains is too compact to thread onto any CNT of the dimensions considered in this study.

Adsorption of a single peptide

As mentioned in the Methods section, when the peptide adopted structures such that the sulfurs were closer than 15 Å for sustained periods of the production trajectory (*i.e.* had not gone beyond the retraction threshold for more than 0.5 ns at one time), these structures were considered to be capable of forming a disulfide bond; these structures are referred to as 'cyclised' from now on. Initially, crossbar and co-linear configurations of RC5

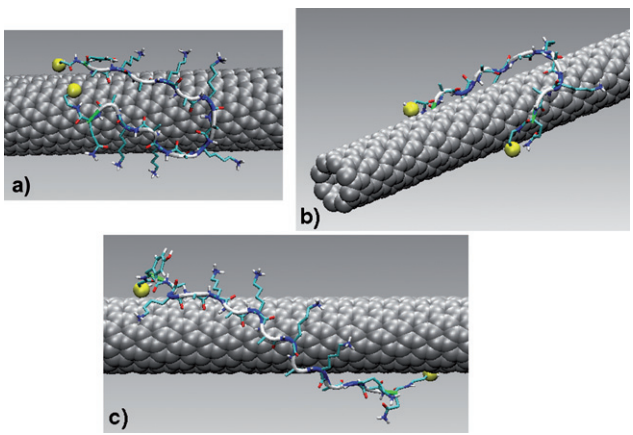

Fig. 4 Example snapshots of typical conformations for the single peptide chain adsorbed on the CNT surface. (a) atop-cyclised, (b) half-wrap, (c) atop-extended. The relative size of the sulfur atoms (yellow) is increased for clarity.

and RC7 were investigated in contact with a single CNT (of all diameters in the range mentioned in the Methods section). Spontaneous wrapping of the peptide was not seen to occur on the timescale of these simulations (~10 ns), and in many cases the peptides formed a cyclised/hairpin structure on the surface of the nanotube, denoted herein as an 'atop-cyclised' structure. Other common conformations found included a 'half-wrap' structure where the peptide formed a rough semi-circle around the CNT, and an 'atop-extended' structure where the peptide adsorbed on the CNT in an extended conformation with the long axis of the backbone and CNT roughly aligned. An example of each of these three types of adsorbed structure is shown in Fig. 4.

For simulations started with the peptide in a cyclised-wrap initial configuration, none of the peptides resulted in a stable 'cyclised' conformation that persisted for more than 2 ns. The retraction times for each of the studied peptide–CNT combinations are given in Table 1. These results indicate that the situation where the peptide (either RC5 or RC7) completely encircles the CNT is at the very best *marginally* more stable for a limited range CNT diameters; D_a = 0.45–0.65 nm for RC5, and D_a = 0.85–1.15 nm for RC7. However, in only one of these systems did the cyclised-wrap structure consistently persist for more than 1 ns (RC5 on the D_a = 0.45 nm CNT), as evidenced by the sulfur–sulfur non-bonded contact distance and percentage of radial coverage, both plotted against time and shown in Fig. 5.

To further investigate the possibility of forming stable, cyclised-wrap structures, we used additional initial configurations where the sulfur atoms in cyclised-wrap geometry were treated as bonded. Our intention here was to check that by initially relaxing the bonded-wrap configuration, we could obtain a more stable system once the disulfide bond was cut (and hydrogens added). We performed these simulations only for the RC5 peptide on the D_a = 0.75 nm tube. The resulting conformation of the bonded-wrapped peptide was distorted such that a rough polygonal shape formed from the initial circular shape. After 1.5 ns the disulfide bond was cut and the simulation continued. Again, the cyclised-wrap conformation did not persist, with the sulfur atoms retracting to beyond 15 Å separation within an average of 268 ps. While this is an improvement on the average retraction time in the non-bonded case (sulfur–sulfur contact persisted on average for almost four times as long), these data still suggested that the cyclised-wrap conformation is not highly stable, at least for most tube diameters, irrespective of the initial conditions used here.

Table 1 Initial time taken (ps) for the sulfur–sulfur non-bonded contact in the circular-wrap cyclised initial configuration to extend beyond 15 Å and remain so for at least 0.5 ns, for a range of CNT diameters, D_a (nm)

Peptide	D_a/nm	Run 1/ps	Run 2/ps
RC5	0.45	1940	1867
RC5	0.55	283	174
RC5	0.65	767	860
RC5	0.75	40	103
RC5	0.85	371	63
RC7	0.75	152	34
RC7	0.85	830	14
RC7	0.95	130	166
RC7	1.05	494	481
RC7	1.15	335	405
RC7	1.25	182	134

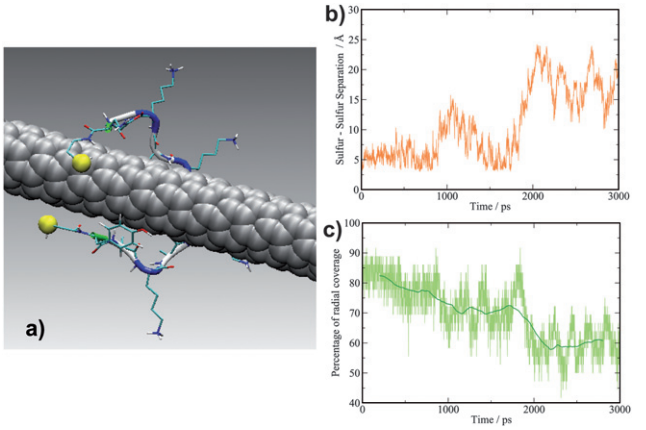

Fig. 5 (a) Snapshot (taken at 1 ns) of the RC5 peptide in aqueous solution maintaining a cyclised-wrap conformation up to around 2 ns. The relative size of the sulfur atoms (yellow) is increased for clarity. (b) Plot of sulfur–sulfur non-bonded intra-peptide distances as a function of time. (c) Plot of percentage of radial coverage as a function of time. The dark line indicates the running average of this coverage.

Adsorption of two peptides

We start by presenting our results for the dimer starting configuration. In these cases, a much greater degree of stability was noted for a greater range of CNT diameters compared with that for the single peptide simulations, with both pairs of sulfur–sulfur non-bonded contacts staying within 15 Å for much longer periods of time, as summarised in Table 2. For the dimer initial configuration, the greatest stabilities were noted for the RC5 peptide on the D_a = 0.75 nm CNT, with both pairs of sulfurs remaining in close contact for over 2 ns. The least stability was observed on the D_a = 0.45 nm CNT with RC7, where one pair of sulfur atoms remained in contact for an average of 595 ps. The persistence times for nanotube encapsulation by these peptide dimer motifs clearly exceed those noted for most cases of the single peptide in the circularly-wrapped configuration. This distribution of persistence times with tube diameter is in broad alignment with the experimental observations of Ortiz-Acevedo *et al.*;[12] dimers of the RC5 peptide persisted for longer on the D_a = 0.45 nm and 0.75 nm CNTs, while the RC7 dimers showed better stability on the D_a = 0.75 nm and 1.15 nm CNTs. While the dimer motif shows a greater stability compared with the single-chain cyclised-wrap motif, we acknowledge that even the dimer arrangement did not show exceptionally high stability, usually fragmenting within 2 ns or less.

Table 2 Initial time taken (ps) for the sulfur–sulfur non-bonded contacts (denoted C1 and C2) in the dimer initial configuration to extend beyond 15 Å and remain so for at least 0.5 ns, for a range of CNT diameters, D_a (nm). A star indicates a contact persisted for the entire trajectory

Peptide	D_a/nm	C1/C2 Run 1/ps	C1/C2 Run 2/ps
RC5	0.45	1279/4000*	1946/4000*
RC5	0.75	2423/2104	2289/740
RC5	1.15	698/3000*	869/4000*
RC7	0.45	260/5000*	930/4000*
RC7	0.75	1840/5000*	1590/2210
RC7	1.15	1582/5000*	1149/1249

Interestingly, it was noted that in almost all of the twelve production runs for the dimer analysed here, *one* of the two sulfur–sulfur non-bonded contacts remained within 15 Å for the entire trajectory (typically 4–5 ns). Therefore, our measure of dimer stability essentially probes the amount of time it takes for the first sulfur–sulfur contact to retract. However, upon a number of occasions, it was noticed that even when one of the sulfur–sulfur contacts had retracted, substantial contact between three of the four sulfurs remained; suggesting that the two peptide chains stayed reasonably close to each other, albeit not strictly in a dimer configuration. For example, in one of our RC5/0.45 nm runs, two inter-penetrating half-wrap configurations formed, such that the radial coverage of the CNT was almost complete (*i.e.* the radial coverage of one of the chains covered a region of the CNT that was complementary with the coverage provided by the other chain), even though one of the sulfur–sulfur contacts had formally retracted. A snapshot of this configuration, plus plots of the percentage radial coverage, and also the sulfur–sulfur contacts, as a function of time, are given in Fig. S2 of the ESI.† A more common situation was that one chain formed a pseudo-atop-cyclised geometry, while the other chain formed a half-wrap or atop-extended geometry, with one chain end of the latter interacting with the two chain ends of the former. Such an example, again for the RC5/0.45 nm system, is shown in Fig. S3 of the ESI†, where a snapshot of this configuration, plus plots of the percentage radial coverage, and also the sulfur–sulfur contacts, as a function of time, are given.

This '3-sulfur' stabilisation appeared for both of the RC5/0.45 nm cases, both of the RC5/1.15 nm cases, both of the RC7/0.45 nm cases and one each of the RC7/0.75 nm and RC7/1.15 nm cases. However, good performance in terms of percentage of radial coverage was only found for the RC5/0.45 nm, RC7/0.45 nm and RC7/0.75 nm systems. Therefore, radial coverage did persist in several of the above cases typified by 3-sulfur interactions; these data suggest that such 3-sulfur conformations may be stable upon formation of a single, inter-chain disulfide bond. As demonstrated in the ESI,† these 3-sulfur conformations that supported good radial coverage persisted for much longer (typically 3–4 ns) than either the dimer or single-chain cyclised-wrap geometries.

One exception to the 3-sulfur stabilisation noted for many of our trajectories was found for the RC7 peptide on the D_a = 0.75 nm CNT. In this case both the dimer inter-chain contacts broke by around 2.5 ns, yielding two separate adsorbed chains. During this process, one of these chains spontaneously formed a cyclised-wrap structure that persisted for a further 4 ns. Data confirming the persistence of this structure are given in Fig. S4 of the ESI. This event is in contrast with the results of our previous cyclised-wrap single-chain simulations, which suggested the RC7/0.75 nm system was not stable to CNT encapsulation. Further work will be required to probe if the event reported here is extremely rare; *e.g.* it is possible that the formation mechanism of this cyclised-wrap structure necessarily involves a second peptide chain (*vide infra*). In summary, our results suggest a possible selectivity for those nanotubes with a circumference that can be bridged by two adsorbed peptide chains, usually where at least one of which maintains a 'half-wrap' geometry. However, we note that while the dimer configuration appears reasonably stable when simulations are started in this geometry, we have not explored all possible mechanisms of formation of this dimer complex.

Table 3 Initial time taken (ps) for the sulfur–sulfur non-bonded contact in the helical initial configuration to extend beyond 15 Å and remain so for at least 0.5 ns, for a range of CNT diameters, D_a (nm). A star indicates a contact persisted for the entire trajectory

Peptide	D_a/nm	Run 1/ps	Run 2/ps
RC5	0.45	16	69
RC5	0.75	8500*	123
RC5	1.15	579	98
RC7	0.45	1619	2233
RC7	0.75	196	197
RC7	1.15	879	1253

We next discuss the helical-wrapped simulation results. Overall, simulations started in this type of initial configuration did not remain in stable helical geometries. Of the 12 production runs we analysed, 10 resulted in geometries comprising two, separate peptide chains adsorbed on the CNT surface, without any close contact between non-bonded sulfurs. The retraction times for the initial sulfur–sulfur contact, summarised in Table 3, indicate a stability that is intermediate between the single-chain cyclised-wrap initial configuration (Table 1) and the two-chain dimer initial configuration (Table 2), although there appears to be a good deal of variation in these retraction times. However, the retraction times in Table 3 must be balanced against other data such as the percentage of radial coverage. For example, while one of the RC5/1.15 nm systems showed over 0.5 ns of inter-chain sulfur–sulfur contact, this arrangement of the chains could not encapsulate the CNT (the percentage of radial coverage was too low, even in the ideal helical initial arrangement). However, we noted in this instance that in the resulting final geometry, while not supporting any close sulfur–sulfur contacts, the chains themselves were arranged side-by-side on the surface, covering distinct radial portions of the CNT, such that a third such chain might have been accommodated. In this case a third chain would have completed full radial coverage of the CNT, reminiscent of the CNT coverage results reported by Nish *et al.*[22] using PFO, although in our case *three* close inter-chain contacts would need to have been formed and maintained. However, we propose that the likelihood of forming such a trimer complex would be much smaller (based on the presumably smaller chance of encounter) than that for forming a two-chain complex, at least at peptide low concentrations. It is suggested therefore that this type of encapsulation might be more appropriate for solutions with high peptide concentration.

As mentioned above, there were a few exceptions to the outcome where the helix configuration ultimately disintegrated into separate adsorbed chains on the CNT surface. The first exception is the RC5/0.45 nm case, where the sulfur–sulfur contact retracted almost instantly (16 ps). However, for an intermediate period in this trajectory, one of the chains formed a cyclised-wrap configuration that was sustained from around 1–4 ns. The second chain was not involved in assisting the maintenance of the cyclised-wrap peptide. Both the intra-chain sulfur–sulfur distance and the percentage radial coverage plots are shown in Fig. S5 of the ESI.† These results again emphasise that cyclised-wrap conformations can be favoured for RC5 on the D_a = 0.45 nm CNT, provided the initial configuration is

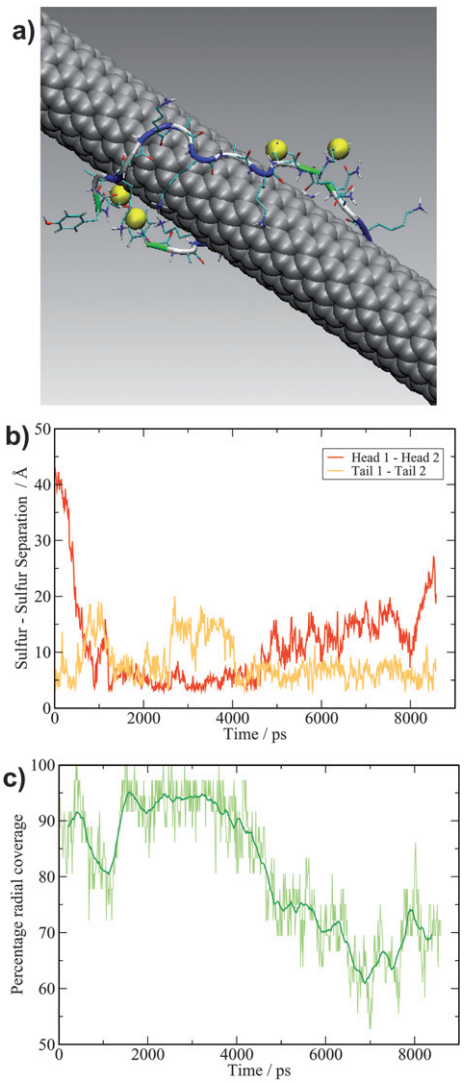

Fig. 6 (a) Snapshot of the RC5/0.75 nm system in aqueous solution maintaining a dimer conformation (taken at 1 ns), started from a helix initial configuration. The relative size of the sulfur atoms (yellow) is increased for clarity. (b) Plot of sulfur–sulfur non-bonded inter-peptide distances as a function of time. (c) Plot of percentage of radial coverage as a function of time. The dark line indicates the running average of this coverage.

sufficiently close to a circle; in the initial geometry the helical winding for the 0.45 nm tube results in a tightly-curved peptide chain. The narrow diameter of the $D_a = 0.45$ nm CNT also yielded an exceptional case, this time for the RC7 peptide. Actually, these were the only production runs where a helical geometry was seen to persist for any period of time beyond 1.5 ns (1619 ps and 2233 ps respectively), as evidenced by the plots of sulfur–sulfur distance and percentage radial coverage with time (Fig. S6 of the ESI†) for the latter of these two cases. In this particular example, following the collapse of this helix structure, this system rearranged into a 3-sulfur configuration, such that a new inter-chain contact formed between the atop-extended geometry of chain 2, and the half-wrap geometry of chain 1. Our final exception was found for the mid-range tube diameter of $D_a = 0.75$ nm, with the RC5 peptide. In this case, the initial sulfur–sulfur non-bonded contact persisted for the entire trajectory (8.5 ns). However, the initially helical geometry of the chains quickly rearranged into a dimer conformation (by around 60 ps). This dimer arrangement was maintained until around the 6.5 ns mark, at which point the non-helix inter-chain contact retracted. A snapshot of this dimer conformation, along with plots against time of the inter-chain contacts and the percentage radial coverage are shown in Fig. 6.

From a comparison of the relative initial stabilities of the dimer and helix configurations, and also the cyclised-wrap single chain simulations, we infer that, for all but the smallest CNT diameters, the presence of two inter-chain contacts appears to ensure that at least one of these contacts persists for longer periods of time, as was the case for the dimer initial geometry. On the other hand, most of the helix initial geometries did not form lasting inter-chain contacts, nor did most of the cyclised-wrap initial geometries; both start with a single sulfur–sulfur contact. Moreover, the fact that we noted formation of cyclised-wrap and dimer conformations arising from *helical* initial geometries adds further weight to our existing findings; that cyclised-wrap geometries can be supported by the smaller diameter CNTs, and that dimer geometries can be supported by the mid-sized to large diameter CNTs.

Finally, we report on our simulations where we modelled two cyclised-wrap chains side-by-side, in this case only for the RC7 peptide on the $D_a = 0.75$ nm CNT. These simulations were performed as an initial investigation into whether the presence of an additional chain can stabilise a cyclised-wrap geometry. For two of our three production runs, the initial times taken for the original intra-chain sulfur–sulfur distances to retract was found to be: 362 ps/1260 ps (trajectory of 5 ns duration) and 4381 ps/5000 ps (trajectory of 6 ns duration) respectively. In the former case, one chain quickly rearranged into a half-wrap conformation, with an inter-chain contact formed with the remaining cyclised-wrap geometry (which held for almost 1.3 ns). Ultimately this trajectory resulted in two inter-penetrating half-wrap geometries, with complementary radial coverage of the CNT; disulfide bond formation would yield 100% CNT encapsulation for this system (data given in Fig. S7 of the ESI†). This is similar to what was seen for one of the RC5/0.45 nm dimer geometries. For our second production run, both cyclised-wrap geometries held for over 4 ns, then collapsed to a half-wrap geometry and an atop-adsorbed geometry (not denoted as atop-extended because it contains a tight turn, *vide infra*), connected by a single inter-chain contact. However, radial coverage dropped below 65% by the end of this trajectory. The final production run was atypical in that both the intra-chain distances retracted quickly, but consequently oscillated into and out of range for the remainder of the trajectory, with contacts persisting for 0.5–1 ns before retracting again, *etc.* In all of our production simulations reported here, this was the only case where oscillating contact was seen to take place. As such, we regard retraction times to be not meaningful in this case.

These data appear to suggest that the presence of a second nearby chain can indeed prolong the timescale over which a cyclised-wrap conformation can be stable (and therefore could, if oxidised, encapsulate a CNT), at least for the RC7/0.75 nm system. The retraction times noted for this double cyclised-wrap case are an order of magnitude longer than for the single-chain case (see Table 1 for comparative single-chain times). Although

based on our single-chain results we consider it somewhat unlikely that two cyclised-wrap chains would spontaneously form in a side-by-side arrangement, this adds weight to our proposal, mentioned above, that a single cyclised-wrap chain *might* be stabilised by the presence of another peptide chain (regardless of conformation of this second chain).

Discussion

Although these simulation data show broad agreement with experiment, a mention of some limitations of our approach is warranted. Despite our extensive exploration of initial conditions, and the duration of our production runs, we cannot guarantee that we have located *all* important configurations of these systems. Therefore, caution in interpretation of these results, as a complete representation of equilibrium conditions, is necessary. Additionally, while the *possibility* of disulfide bond formation was explored here, we have not investigated the actual formation process of these bonds. While beyond the scope of this paper, it would be interesting to investigate if the action of the oxidising agent was influenced by the presence of the nanotube in this process.

Our findings suggest that complexes involving two peptide chains play a more significant role in explaining the limited diameter selectivity in solubilisation of CNTs. Not only do dimer geometries appear to form comparatively more stable conformations capable of sustaining CNT encapsulation upon oxidation; our evidence indicates stable two-chain configurations based on mixtures of *connected* single-chain adsorption motifs (*e.g.* half-wraps, atop-cyclised and atop-extended geometries) may also be capable of fully wrapping CNTs upon formation of a combination of either intra-peptide or inter-peptide disulfide bonds. Based on our simulations for RC5, the CNT diameters that were seen to support the possibility of sustained CNT encapsulation ranged from $D_a = 0.45$ nm to $D_a = 0.75$ nm. The upper end of this range is attributed to two-chain complex formation, and the lower end is attributed mostly to single-chain cyclised wrap geometries. This range corresponds with $D_v = 0.8$–1.1 nm, in good alignment with the most likely diameters reported by Ortiz-Acevedo *et al.*[12] For our RC7 simulations, the CNT diameters most likely to support tube encapsulation ranged from $D_a = 0.45$–1.15 nm. This range corresponds with $D_v = 0.8$–1.5 nm, again in broad agreement with the most likely diameters reported by Ortiz-Acevedo *et al.*[12] We note that the range of highly-likely diameters for RC5 reported by Ortiz-Acevedo *et al.* is narrower than the range reported for RC7; our simulation data also show this trend.

The maxima in the *consistent* retraction times for both RC5 and RC7 presented in Table 1 may be interpreted *via* a very simple model of polygonal wrapping. It was noticed in most instances of sustained cyclised-wrap trajectories that the peptide backbone did not form a smoothly curving arc, but rather formed a segmented polygon around the CNT, as shown in Fig. 7(a). The segments of these polygons ran the length of the Lys-to-Lys distance along the backbone, often (but not always) with the Lys appearing at the polygon corners. This segment length is around 7 Å. In an idealised case, the RC5 peptide then comprises five segments of around 7 Å in length each; similarly, the idealised RC7 peptide comprises seven such segments. One can then consider various cases of a polygon wrapping a circle,

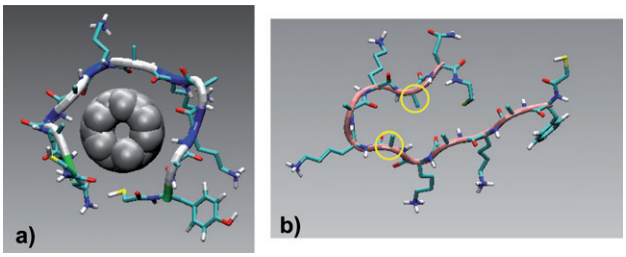

Fig. 7 (a) Snapshot of the RC5/0.45 nm system in aqueous solution showing an example of polygonal wrapping (in this case a pentagon). (b) Snapshot of a typical α-turn conformation for the example of the RC5/85 nm system (tube not shown). The sixth and tenth α-carbons are indicated with yellow circles.

e.g. pentagon, hexagon, heptagon, *etc.*, with edge sides of 7 Å (or 14 Å), and from this infer which CNT diameter would support such idealised wrapping. For example, the ideal pentagonal (full) wrap of a CNT by RC5 would be supported by $D_a = 0.44$ nm. An incomplete hexagonal wrap of a CNT (leaving a 7 Å distance between chain ends) by RC5 would be supported by $D_a = 0.69$ nm. Similarly, the ideal heptagonal (full) wrap of a CNT by RC7 would be supported by $D_a = 0.93$ nm, and an incomplete octagonal wrap by $D_a = 1.17$ nm. These dimensions are in broad (but not perfect) alignment with the range of diameters which *consistently* showed longer retraction times in each case. While at present we do not have an explanation for this segmented-chain behaviour of the peptide conformation, we speculate that the regular spacing of the charged moieties may play a role here. If this is the case, the spacing between the charged groups (and therefore the 'segment length') could be a useful variable in peptide design, perhaps in relation to the radius of the tube to be encapsulated. Further, this spacing need not be uniform—perhaps tubes of different chirality could be encapsulated with better selectivity with judicious design of non-uniform segment lengths. Another way in which the peptide encapsulation may be improved could be *via* incorporation within each segment of L-chiral residues that are known to show affinity for nanotubes, such as tryptophan.[9,23]

Finally, we point out a feature of many of the resulting adsorbed conformations for both RC5 and RC7 (whether interacting *via* an inter-chain contact or not). In the Results section, we mentioned that the peptide in solution (without the presence of a CNT) showed a propensity to form a tight β-turn part-way along the chain. Interestingly, no such β-turns were noted for any of our adsorbed peptide chains. Instead, many instances of an α-turn part-way along the chain were noted; defined here to be a tight turn where C^α carbons separated by four peptide bonds were in close (< 7 Å) non-bonded contact. An example of this α-turn conformation is shown in Fig. 7(b). These turns were very stable, often lasting for the rest of the entire trajectory, once formed (*e.g.* typically between 3–5 ns). We also noted the formation of ω-loops on a number of occasions. We do not yet have an explanation for why the type of tight-turn would change in moving from the free to adsorbed peptide. In any case, at first sight the formation of the α-turns/ω-loops does not appear critical to CNT encapsulation. While we are aware of simulations that have probed *large* changes in peptide secondary structure upon adsorption onto a surface,[45–47] we are not aware

of any report of the subtle changes in secondary structure as noted in this work.

Conclusions

Molecular dynamics simulations were used to explore the encapsulation behaviour of reversible cyclic peptides adsorbed onto single-walled carbon nanotubes. Our findings suggest that except for the RC5 chain adsorbed on the $D_a = 0.45$ nm diameter tube, complete CNT wrapping due to single-peptide cyclisation did not appear to be the most likely mode of encapsulation. Instead, our results indicate that the formation of both intra-peptide and inter-peptide disulfide bonds may be responsible for the limited diameter selectivity in CNT solubilisation seen in the experiments reported by Ortiz-Acevedo *et al.*[12] The range of CNT diameters found by simulation to support likely CNT encapsulation is in very good agreement with the experimentally-determined diameters. The two-chain complexes noted in this work appeared to comprise mixtures of the single-chain adsorbed motifs linked by at least one inter-chain contact. Cyclised-wrap geometries were indicated to be more stable when in the presence of a second peptide chain. The variation in stability of the cyclised-wrap conformation, as measured by time taken for the initial sulfur–sulfur contact to retract, could be broadly explained by using a very simple model of polygonal wrapping of a segmented chain around a circle. The findings presented here should help with the future optimisation and design of peptides with enhanced selectivity for specific CNT diameters.

Acknowledgements

The authors gratefully acknowledge the computing facilities of the Centre for Scientific Computing, University of Warwick. SRF and TRW thank the EPSRC for a summer vacation bursary. We acknowledge funding from EPSRC (EP/E02095X/1) for resources used to carry out this work.

References

1 K. H. Park, M. Chhowalla, Z. Iqbal and F. Sesti, *J. Biol. Chem.*, 2003, **278**, 50212–50216.
2 R. H. Baughman, A. A. Zakhidov and W. A. de Heer, *Science*, 2002, **297**, 787–792.
3 K. A. Drouvalakis, S. Drouvalakis, W. Heuber, L. G. Kozar, P. J. Utz and H. Dai, *Biosens. Bioelectron.*, 2008, **23**, 1413–1421.
4 X. Liu, L. Shi, W. Niu, H. Li and G. Xu, *Biosens. Bioelectron.*, 2008, **23**, 1887–1890.
5 B. L. Allen, P. D. Kichambare and A. Star, *Adv. Mater.*, 2007, **19**, 1439–1451.
6 N. Shao, E. Wickstrom and B. Panchapakesan, *Nanotechnology*, 2008, **19**, 465101.
7 S. Dhar, Z. Lin, J. Thomale, H. J. Dai and S. J. Lippard, *J. Am. Chem. Soc.*, 2008, **130**, 11467–11476.
8 V. C. Moore, M. S. Strano, E. H. Haroz, R. H. Hauge, R. E. Smalley, J. Schmidt and Y. Talmon, *Nano Lett.*, 2003, **3**, 1379–1382.
9 S. Wang, E. S. Humphreys, S.-Y. Chung, D. F. Delduco, S. R. Lustig, H. Wang, K. N. Parker, N. W. Rizzo, S. Subramoney, Y.-M. Chiang and A. Jagota, *Nat. Mater.*, 2003, **2**, 196–200.
10 G. R. Dieckmann, A. B. Dalton, P. A. Johnson, J. Razal, J. Chen, G. M. Giordano, E. Muñoz, I. H. Musselman, R. Baughman and R. K. Draper, *J. Am. Chem. Soc.*, 2003, **125**, 1770–1777.
11 V. Zorbas, A. Ortiz-Acevedo, A. B. Dalton, M. Yoshida, G. R. Dieckmann, R. K. Draper, R. H. Baughman, M. Jose-Yacaman and I. H. Musselman, *J. Am. Chem. Soc.*, 2004, **126**, 7222–7227.
12 A. Ortiz-Acevedo, H. Xie, V. Zorbas, W. M. Sampson, A. B. Dalton, R. H. Baughman, R. K. Draper, I. H. Musselman and G. R. Dieckmann, *J. Am. Chem. Soc.*, 2005, **127**, 9512–9517.
13 L. S. Witus, J.-D. R. Rocha, V. M. Yuwono, S. E. Paramonov, R. B. Wilson and J. D. Hartgerink, *J. Mater. Chem.*, 2007, **17**, 1909–1915.
14 K. Saito, V. Troiani, H. Qiu, N. Solladiè, T. Sakata, H. Mori, M. Ohama and S. Fukuzumi, *J. Phys. Chem. C*, 2007, **111**, 1194–1199.
15 E. J. Becraft, A. S. Klimenko and G. R. Dieckmann, *Biopolymers*, 2009, **92**, 212–221.
16 H. Yang, S. C. Wang, P. Mercier and D. L. Atkins, *Chem. Commun.*, 2006, 1425–1427.
17 W. Yi, A. Malkovskiy, Q. Chu, A. P. Sokolov, M. L. Colon, M. Meador and Y. Pang, *J. Phys. Chem. B*, 2008, **112**, 12263–12269.
18 M. S. Arnold, A. A. Green, J. F. Hulvat, S. I. Stupp and M. C. Hersam, *Nat. Nanotechnol.*, 2006, **1**, 60–65.
19 N. R. Tummala and A. Striolo, *ACS Nano*, 2009, **3**, 595–602.
20 X. Tu, S. Manohar, A. Jagota and M. Zheng, *Nature*, 2009, **460**, 250–253.
21 S.-Y. Ju, J. Doll, I. Sharma and F. Papadimitrakopoulos, *Nat. Nanotechnol.*, 2008, **3**, 356–362.
22 A. Nish, J. Hwang, J. Doig and R. J. Nicholas, *Nat. Nanotechnol.*, 2007, **2**, 640–646.
23 S. D. Tomásio and T. R. Walsh, *Mol. Phys.*, 2007, **105**, 221–229.
24 Y. Cheng, G. R. Liu, C. Lu and D. Mi, *J. Phys. D: Appl. Phys.*, 2008, **41**, 055308.
25 J. W. Shen, T. Wu, Q. Wang, Y. Kang and X. Chen, *ChemPhysChem*, 2009, **10**, 1260–1269.
26 C. C. Chiu, G. R. Dieckmann and S. O. Nielsen, *J. Phys. Chem. B*, 2008, **112**, 16326–16333.
27 Y. Kang, Y. C. Liu, Q. Wang, J. W. Shen, T. Wu and W. J. Guan, *Biomaterials*, 2009, **30**, 2807–2815.
28 C. C. Chiu, G. R. Dieckmann and S. O. Nielsen, *Biopolymers*, 2009, **92**, 156–163.
29 S. M. Tomásio and T. R. Walsh, *J. Phys. Chem. C*, 2009, **113**, 8778–8785.
30 H. Xie, E. J. Becraft, R. H. Baughman, A. B. Dalton and G. R. Dieckmann, *J. Pept. Sci.*, 2008, **14**, 139–151.
31 C. G. Salzmann, M. A. H. Ward, R. M. J. Jacobs, G. Tobias and M. L. H. Green, *J. Phys. Chem. C*, 2007, **111**, 18520–18524.
32 *Tinker – software tools for molecular design.* J. W. Ponder, P. Ren, R. V. Pappu, R. K. Hart, M. E. Hodgson, D. P. Cistola, C. E. Kundrot, and F. M. Richards; Washington University School of Medicine, version 4.2 ed., 2004.
33 *The gromos96 manual and user guide*. W. F. van Gunsteren, S. R. Billeter, A. A. Eising, P. H. Hünenberger, P. H. Krüger, A. E. Mark, W. R. P. Scott, and I. G. Trioni; Hochschulverlag AG an der ETH Zürich, Zürich, Switzerland, 1996.
34 H. J. C. Berendsen, D. van der Spoel and R. van Drunen, *Comput. Phys. Commun.*, 1995, **91**, 43–56.
35 E. Lindahl, B. Hess and D. van der Spoel, *J. Mol. Model.*, 2001, **7**, 306–317.
36 D. van der Spoel, E. Lindahl, B. Hess, G. Groenhof, A. E. Mark and H. J. C. Berendsen, *J. Comput. Chem.*, 2005, **26**, 1701–1719.
37 H. J. C. Berendsen, J. P. M. Postma, W. F. van Gunsteren, J. Hermans, and B. Pullman, in *Intermolecular Forces*, ed. B. Pullman, Reidel Publishing Company, Dordrecht, 1981, pp. 331–342.
38 S. Nosé, *J. Chem. Phys.*, 1984, **81**, 511–519.
39 S. Nosé, *Mol. Phys.*, 1984, **52**, 255–268.
40 W. G. Hoover, *Phys. Rev. A: At., Mol., Opt. Phys.*, 1985, **31**, 1695–1697.
41 U. Essmann, L. Perela, M. L. Berkowitz, T. Darden, H. Lee and L. G. Pedersen, *J. Chem. Phys.*, 1995, **103**, 8577–8592.
42 C. T. White, D. H. Robertson and J. W. Mintmire, *Phys. Rev. B: Condens. Matter*, 1993, **47**, 5485–5488.
43 *tubebash*. R. G. A. Veiga; Universidade Federal de Uberlandia, Brazil, 2005.
44 W. Humphrey, A. Dalke and K. Schulten, *J. Mol. Graphics*, 1996, **14**, 33–38.
45 M. Mijajlovic and M. J. Biggs, *J. Phys. Chem. C*, 2007, **111**, 15839–15847.
46 L. A. Capriotti, T. P. Beebe and J. P. Schneider, *J. Am. Chem. Soc.*, 2007, **129**, 5281–5287.
47 H. Heinz, B. L. Farmer, R. B. Pandey, J. M. Slocik, S. S. Patnaik, R. Pachter and R. R. Naik, *J. Am. Chem. Soc.*, 2009, **131**, 9704–9714.

